THE JOURNAL OF BIOLOGICAL CHEMISTRY VOL. 282, NO. 15, pp. 11213–11220, April 13, 2007

Conserved Structural and Functional Properties of D-domain Containing Redox-active and -inactive Protein Disulfide Isomerase-related Protein Chaperones*

Received for publication, May 9, 2006, and in revised form, February 7, 2007 Published, JBC Papers in Press, February 12, 2007, DOI 10.1074/jbc.M604440200

Undine Lippert[‡], **Daojun Diao**[§1], **Naomi N. Barak**[§1], **and David M. Ferrari**[§¶2]

From the [‡]*Department of Neurobiology, Max-Planck Institute for Biophysical Chemistry, Am Fassberg 11, 37077 Goettingen, Germany,* [§]*Max-Planck Research Unit for Enzymology of Protein Folding, Weinbergweg 22, 06120 Halle (Saale), Germany, and* [¶]*Department of Cardiology and Pneumology, Georg-August University Goettingen, Robert-Koch-Strasse 40-44, 37075 Goettingen, Germany*

The structure and mode of binding of the endoplasmic reticulum protein disulfide isomerase-related proteins to their substrates is currently a focus of intensive research. We have recently determined the crystal structure of the *Drosophila melanogaster* protein disulfide isomerase-related protein Wind and have described two essential substrate binding sites within the protein, one within the thioredoxin b-domain and another within the C-terminal D-domain. Although a mammalian ortholog of Wind (ERp29/28) is known, conflicting interpretations of its structure and putative function have been postulated. Here, we have provided evidence indicating that ERp29 is indeed similar in both structure and function to its *Drosophila* ortholog. Using a site-directed mutagenesis approach, we have demonstrated that homodimerization of the b-domains is significantly reduced *in vitro* upon replacement of key residues at the predicted dimerization interface. Investigation of Wind-ERp29 fusion constructs showed that mutants of the D-domain of ERp29 prevent transport of a substrate protein (Pipe) in a manner consistent with the presence of a discrete, conserved peptide binding site in the D-domain. Finally, we have highlighted the general applicability of these findings by showing that the D-domain of a redox-active disulfide isomerase, from the slime mold *Dictyostelium discoideum*, can also functionally replace the Wind D-domain *in vivo*.

Within the endoplasmic reticulum (ER),[3] an optimal protein folding environment (1) essential for many secretory proteins is provided by a battery of ER chaperones and folding factors, including the chaperones calnexin/calreticulin (2), the Hsp70 homolog immunoglobulin heavy chain binding protein (BiP), and the protein disulfide isomerase (PDI)-related family of redox enzymes and chaperones (3, 4).

PDI-related proteins have various functions (5), including redox and chaperone activities, regulation of calcium homeostasis, and regulation of protein export from the ER for degradation. Although relatively much is known about the respective mechanisms of chaperone action of the calnexin/calreticulin proteins and BiP (6–9), less is known about the detailed molecular basis of PDI-chaperone activity. This is, to a significant extent, due to the weak character of PDI-substrate interactions. Thus, although it is now known that not only the chaperone function of these proteins but to varying extents their redox activity as well relies on their non-covalent interaction with substrate proteins (4, 10–13), our knowledge of peptide specificity, peptide binding sites, or the molecular basis for the observed substrate selectivity of these proteins remains sketchy.

Redox activity and chaperone function of PDI proteins requires interaction with substrates. The principle peptide binding site in PDI has been mapped to the b′-domain, although contributions from other domains occur (12). Thus, much attention has been focused on the redox-inactive domains. Recently, peptide binding sites in the b-domains of PDI, ERp57, and the ERp29 ortholog Wind have been described (14–16). Interestingly, these binding sites all map to a region close to what would be the catalytically active redox-active sites in the a and a′ domains of PDI.

The first crystal structure of a complete PDI family member of the eukaryotic ER was determined in 2003 (13), allowing a direct structural interpretation of the peptide-binding sites. This *Drosophila melanogaster* protein, Wind, contains an N-terminal thioredoxin b-type domain found in most PDI-related proteins as well as a unique C-terminal domain (the D-domain) found only in the PDI-D group of PDI-related proteins (3).

The PDI-D proteins comprise two subgroups. PDI-Dα proteins contain one or more redox-active a-type thioredoxin domains, whereas only redox-inactive b-type domains are present in PDI-Dβ proteins. Current knowledge suggests that PDI-Dβ proteins possess chaperone-like activities. Wind is required for export from the ER of an essential Golgi trans-

* This work was funded in part by the Deutsche Forschungsgemeinschaft, the Fonds der Chemischen Industrie, and an Excellence Network of the State of Sachsen Anhalt. The costs of publication of this article were defrayed in part by the payment of page charges. This article must therefore be hereby marked "*advertisement*" in accordance with 18 U.S.C. Section 1734 solely to indicate this fact.

[1] These authors contributed equally to this work.

[2] Present address: Max Planck Research Unit for Enzymology of Protein Folding, Weinbergweg 22, 06120 Halle (Saale), Germany. To whom correspondence should be addressed. Tel.: 49-0345-5522830; Fax: 49-0345-5511972; E-mail: ferrari@enzyme-halle.mpg.de.

[3] The abbreviations and trivial names used are: ER, endoplasmic reticulum; PDI, protein disulfide isomerase; PDI-Dα, D-domain containing PDI-related protein with a redox active a-type thioredoxin domain; PDI-Dβ, D-domain containing PDI-related protein with a redox inactive b-type thioredoxin domain; WT, wild type; GFP, green fluorescent protein; EGFP, enhanced GFP.

membrane proteoglycan-modifying enzyme, Pipe (a 2-*O*-sulfotransferase), which otherwise remains trapped in the ER (8), and human and rat ERp29 (the human protein is also known as ERp28) interact with mutant hepatitis B surface antigen and thyroglobulin, respectively (17, 18).

Interestingly, in *D. melanogaster* Wind, it was shown that substrate-processing activity requires both the b- and D-domains, and a putative peptide binding site has been mapped to each of these domains (13, 14). This identified for the first time, in mammalian PDI-related proteins, a putative peptide-binding site in a domain not related to thioredoxin. Although a mammalian Wind ortholog ERp28/29 cannot replace Wind in Pipe processing, the D-domains of both proteins could be exchanged, indicating functional conservation between the proteins (13). The findings on the Wind protein structure and function are an important milestone in the elucidation of PDI and PDI-D chaperone-substrate interaction mechanisms. However, the general applicability of the findings was unclear, as variant dimerization models for the b-domain and tertiary structures of the D-domains of mammalian orthologs had been suggested (19, 20).

Mkrtchian and colleagues (19) report NMR structures of the individual b- and D-domains of rat ERp29 and claim that residues Asp-71, Phe-118, Arg-122, Asp-123, and Trp-144 are involved in dimerization, whereas residues Gly-67, Glu-68, Gly-97, and Asp-98 may be involved in the formation of higher homo-oligomers. This is in conflict with the findings from our group (13, 14), where the residues identified by crystallographic and biochemical analyses in Wind dimer formation are on the opposite face of Wind and include Gly-26, Val-28, Asp-31, and Lys-41. In addition, Pro-116 (a structurally important residue of the thioredoxin fold) in ERp29 was suggested to have a *trans*-conformation, whereas the corresponding residues in Wind and other PDI proteins clearly have a *cis* conformation (3, 13). Furthermore, the proposed structure of the D-domain of ERp29 deviates dramatically from that of Wind in the relative orientation of helices 8 and 9 to helices 6 and 7, and the cumulative data together with *in vitro* biophysical analysis of ERp29 were interpreted as indicating variant functional roles of the respective proteins (20).

We provide data based on *in vivo* functional assays and *in vitro* molecular characterization showing similarities in structure and function between mammalian ERp29 and its *D. melanogaster* ortholog Wind. Homodimerization of the PDI-D protein, based on association of the thioredoxin b-type domains, occurs via a conserved interface and requires the presence of key residues, the replacement of which reduce dimer formation significantly. For substrates such as Pipe, conservation of function is tightly linked to structural integrity of the D-domain and more precisely to the integrity of a discrete, conserved peptide binding site spanning two structural elements.

In PDI-Dα proteins, identified in yeast and plants, a different domain structure and distribution exists than in PDI-Dβ proteins. Here, two redox-active a-type thioredoxin domains generally precede the D-domain, and b-type domains are absent. In contrast to PDI-Dβ proteins, PDI-Dα proteins are capable of complementing PDI-deficient yeast (13, 21). Furthermore, the PDI-Dα proteins generally lack classical ER retrieval sequences (3, 22), and the degree of similarity between the two subclasses of protein is low (overall ~30% identity between human PDI-Dβ and slime mold PDI-Dα). We show that, despite these differences, the D-domain of a PDI-Dα protein is capable of replacing the D-domain of Wind functionally, suggesting common functional properties among all PDI-D proteins, despite significant evolutionary divergence in primary sequence.

EXPERIMENTAL PROCEDURES

Cell Lines, Bacterial Strains, Plasmids, and Expression Vectors—Mammalian COS-7 and Vero cell lines were obtained from the European Collection of Animal Cell Cultures. *Escherichia coli* XL1-Blue bacterial cells was from Stratagene, the pEGFP-N1 expression vector was from Clontech, and pQE-30 and pQE-60 expression vectors were from Qiagen.

Antibodies—Antibodies against full-length *Drosophila* Wind and human ERp29 were raised as described previously (13, 17). Goat anti-rabbit Cy3-conjugated antibody was from Jackson ImmunoResearch Laboratories.

Bacterial Expression Vector Constructs—D. melanogaster windbeutel full-length cDNA was cloned as described previously (13). For human ERp29, BamHI/HindIII PCR products amplified from pDsb-m28 (17) encoding mature ERp29 were ligated into pQE-30, generating a construct with an N-terminal His_6 tag extension. The ERp29 mutants ERp29-L39D, ERp29-D42N, ERp29-K52S, and the double mutant ERp29-D42N/K52S were made from this construct using standard mutagenesis techniques after recloning into BamHI/NcoI sites of pQE-60. Single domain mouse ERp29 D-domain constructs encoding the complete D-domain and three residues of the linker region (residues Gly-155–Cys-159), harboring the mutations ΔE222 (hereafter referred to as D-ΔE222), E222Q (D-E222Q), A224S/R225A (D-A224S/R225A), R225A (D-R225A), K228E (D-K228E), L229S (D-L229S), or CΔ13 (D-CΔ13), respectively, as well as the WT D-domain (D-WT), were prepared as pQE-30 expression constructs via ligation into the KpnI/HindIII sites. For full-length mouse ERp29, sequences encoding the mature fragments of the WT protein and the mutants ERp29-E222Q, ERp29-R225A/G227S, and ERp29-K228E were created by standard mutagenesis techniques and ligated into BamHI/NcoI sites of pQE-60, generating constructs with a C-terminal His_6 tag.

Mammalian Expression Vector Constructs—Full-length *windbeutel* and Wind-b-p29D, incorporated into the EcoRI/BamHI sites of pEGFP-N1, with a stop codon preceding the enhanced green fluorescent protein (EGFP) sequence (Wind*-EGFP-N1 and Wind-b-p29D*-EGFP-N1) are as described in Ma *et al.* (13) (referred to as Wind and Wind-N-p28D, respectively). Wind-b-p29D point mutants (E222Q, R225A, K228E, L229S, and L242K), double mutant A224S/R225A, the deletion mutants ΔE222 and L242K-CΔ13, as well as the ERp29 thioredoxin domain mutant D42N were constructed using appropriate primers and standard site-directed mutagenesis protocols, using Wind*-EGFP-N1 or Wind-b-p29D*-EGFP-N1 as the template. *Dictyostelium discoideum* Dd-PDI was amplified by PCR from a GFP-Dd-PDI construct (21) and the fragment corresponding to D-domain residues 260–363 fused to the Wind-b cDNA fragment (residues 1–145) generating the vec-

tor Wind-b-DdPDI-D*-EGFP-N1. This construct has an additional 6-residue insert between Wind and the *D. discoideum* Dd-PDI D-domain sequences coding for Glu-Thr, and a 3′ sequence encoding the KEEL retrieval signal.

Cell Culture and Immunofluorescence Assays—COS-7 cells were grown in 90% Dulbecco's modified Eagle's medium and 10% fetal bovine serum with 2 mM L-glutamine and antibiotics at 37 °C in 10% CO_2. Cycloheximide, a protein synthesis inhibitor (Sigma), was applied to the cells 16 h after transfection by electroporation at 0.2 mg/ml for 4 h. For immunofluorescence labeling, the cells were grown on coverslips overnight (16–20 h) and then fixed with 4% paraformaldehyde. Bound Wind antibody, used at a 1:300 dilution, was detected with a 1:1000 dilution of goat anti-rabbit Cy3-conjugated antibody. Visualization of Cy3 and GFP was carried out on an Axiovert 200 microscope (Zeiss) with excitation filters of 565/30 and 480/40 nm, a dichroic beam splitter of 595 and 505 nm, and emission filters of 645/75 and 527/30 nm, respectively.

Protein Expression and Purification—All proteins were expressed in XL1-Blue by induction of A_{600} = 0.7 cultures for 3 h at 37 °C with 1 mM isopropyl-1-thio-β-D-galactopyranoside. Recombinant ERp29 proteins were harvested by sonication of lysozyme-treated cells in pH 8.0 adjusted phosphate-buffered saline or 20 mM Tris-Cl, pH 8.0, 300 mM NaCl, 8 mM imidazole, including 1 mM Pefabloc SC protease inhibitor followed by the addition of Triton X-100 to 0.1% (v/v) and application on a nickel-nitrilotriacetic acid affinity column (Qiagen). Bound protein was washed and eluted as recommended by the manufacturer. Eluted protein was dialyzed against dialysis buffer (10 mM HEPES, pH 7.5, 50 mM NaCl, 1 mM dithiothreitol), concentrated to 15–30 mg/ml, and stored at 4 °C. For far UV circular dichroism measurements, all proteins were further purified by ion exchange chromatography on either Q-Sepharose or S-Sepharose media (GE Healthcare), dependent on protein pI values (data not shown). Protein concentrations were determined with the ProtParam tool (23) using a calculated absorption coefficient at 280 nm. Protein purity was verified by SDS-PAGE.

In Vitro Cross-linking of Recombinant Protein—Purified His_6-tagged ERp29 and Wind proteins were rebuffered in assay buffer (50 mM sodium borate, pH 7.4, 150 mM NaCl). Cross-linking was performed with 0.2 μg/μl protein by the addition of glutaraldehyde to 1% (w/v) followed by quenching after 2 min with 2 M $NaBH_4$. Samples were precipitated with trichloroacetic acid and analyzed by SDS-PAGE.

Biophysical Analysis of ERp29—Far UV circular dichroism spectra were recorded on a Jasco J710 spectrophotometer. All scans at 20 °C were collected as an average of 5–7 scans, whereas temperature gradient scans were repeated 2–3 times. A cell with a path length of 0.1 cm, a scan speed of 50–100 nm/min, a spectral bandwidth of 1.0 nm, and a time constant of 0.5 s for thermal denaturation was used. The maximal high tension voltage was 700 V. All proteins were dialyzed against 20 mM sodium phosphate, pH 7.5, 50 mM NaCl, and 0.01% Triton X-100 before analysis and were used at 11 μM (full-length proteins), 21 μM (single domain construct D-CΔ13), or 19 μM (all other D-domain constructs).

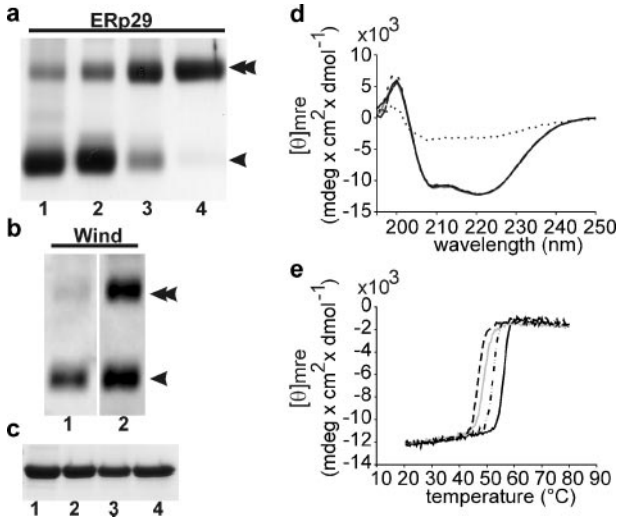

FIGURE 1. **The D42N mutant of human ERp29 interferes with subunit dimerization.** Shown is Coomassie staining of SDS-PAGE gels loaded with bacterially expressed human ERp29. *a*, *lanes 1–4*, ERp29-L39D, D42N, K52S, and WT, respectively. *b*, *Drosophila* Wind D31N (*lane 1*) and WT (*lane 2*). *c*, aliquot of starting material used in *a*. Equal amounts of protein were loaded. Clear differences in the dimerization pattern of ERp29 after cross-linking by glutaraldehyde can be seen. Both WT ERp29 and WT Wind proteins exist to a significant extent as a dimeric species (*double arrow*); for ERp29, the monomeric form is barely detectable (*single arrow*). In contrast, the ERp29-L39D and D42N mutation results in reduced levels of dimer but significant amounts of the monomeric form. This parallels data on the dimerization-impaired Wind-D31N mutant. *d*, far-UV circular dichroism spectra of ERp29-D42N (*gray*), ERp29-K52S (*short dashes*), and ERp29-D42N/K52S (*long dashes*) show that these proteins are similar to WT ERp29 (*black*) in that they retain their secondary structure. In contrast, thermally denatured (55 °C) WT ERp29 (*dotted*) has significantly less ordered structure and shows an altered spectrum. *e*, thermal stability analysis of dimerization mutants ERp29-D42N (*gray*), ERp29-K52S (*short dashes*), and ERp29-D42N/K52S (*long dashes*) as well as WT ERp29. Mean residue ellipticities at 222 nm are plotted as a function of temperature and measured at 0.5 °C intervals.

RESULTS

Dimerization of Human ERp29—The b-domain of Wind includes a homodimerization surface encompassing residues to either side of β1 (residues 24–34), residues within and after α1 (residues 37–43), and residues within and after α2 (residues 70–75) (13). Here, important stabilizing interactions are mediated by Gly-26, Val-28, Asp-31, and Arg-41. Dimerization is critical for the function of Wind, and mutants of Wind that cannot dimerize fail to support Pipe processing (14). Dimerization of Pipe brings the substrate binding site of each b-domain to within ~13 Å of each other, which may be important for chaperone action. In contrast, for rat ERp29, it has been suggested (19) that the dimerization site of rat ERp29 comprises residues Asp-71 (helix α2, corresponds to Wind Glu-60), Phe-118, Arg-122, Asp-123, (within and after strand β4, Wind Ile-108, Lys-112, Gly-113), and Trp-144 (Phe-135 in helix 4 of Wind). The proposed dimerization surfaces are on different faces of the thioredoxin fold. If this were the case, it might also be the reason for the lack of activity of WT ERp29 in the processing of Pipe in our assays (14).

Clearly, a correct interpretation of the mode of dimerization of ERp29 is important for understanding its function *in vivo*, and therefore we chose to analyze participation of residues at the dimerization interface via a mutagenesis approach. In Wind, mutation of Val-28 (V28D) or Asp-31 (D31N) leads to a

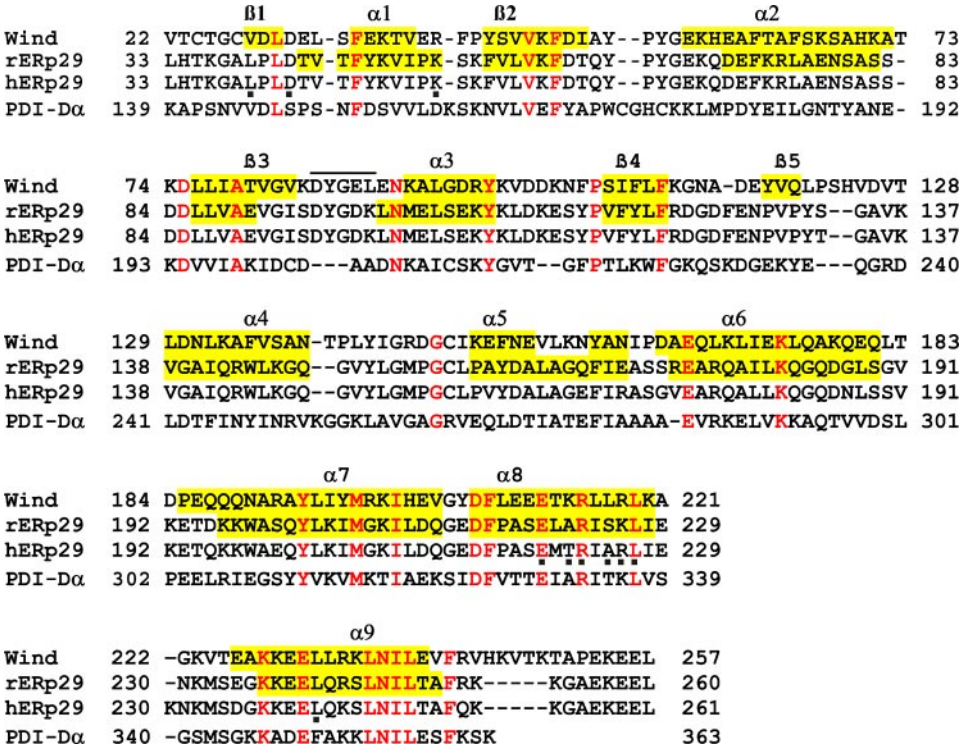

FIGURE 2. **Alignment of PDI-D proteins.** The PDI-Dβ proteins Wind and ERp29 lack redox-active thioredoxin domains but contain a D-domain with weak but significant similarity to the *Dictyostelium* PDI-Dα ortholog. *rERp29*, rat ERp29; *hERp29*, human ERp29; *PDI-Dα*, *D. discoideum* Dd-PDI. *Yellow boxes* indicate experimentally determined secondary structure elements in the Wind and ERp29 sequences. Identical residues are colored *red*, and the corresponding positions in the human ERp29 sequence of residues replaced by mutagenesis are indicated by *dots*. In the b-domain (β1-α4), the *dots* also indicate residues involved in dimerization of ERp29, whereas the *dots* in the D-domain (α5–α9) indicate residues within the substrate binding site of the protein. The region encoding the PDI-D loop, unique to PDI-D proteins, is indicated by a *line*. The linker region connecting the thioredoxin domain and D-domain, in which the conserved (in PDI-Dβ proteins) Cys-159 residue is located, is between α-helices 4 and 5.

significant reduction in dimerization (14), as expected. If mammalian ERp29 proteins have the same structure, mutation of either of the corresponding residues of the human protein, Leu-39 and Asp-42, could have a similar effect. Indeed, as shown in Fig. 1, the dimer:monomer ratio in glutaraldehyde-cross-linked, recombinant ERp29 is significantly shifted toward the monomer for both the L39D and the D42N mutants (Fig. 1*a*, *lanes 1* and *2*, respectively; *single arrow*) compared with the ratio observed for WT protein (Fig. 1*a*, *lane 4*), which is strongly shifted toward dimer formation (*double arrow*). Under the same conditions, the reduction in the proportion of dimer in favor of the monomer can clearly be seen for Wind-D31N, the *Drosophila* equivalent of human ERp29-D42N, compared with the WT protein (Fig. 1*b*, *lanes 1* and *2*, respectively). For ERp29-K52S, dimerization is also impaired, although to a lesser extent (Fig. 1*a*, *lane 3*). We can exclude the possibility that an alternative dimer interface comes into play at altered pH or salt conditions, as our assays were performed under various conditions (pH 6–8, 0–1 M NaCl) with a similar outcome (data not shown).

The D-domain of ERp29 Harbors a Peptide-binding Site Similar to That of Wind—We have previously shown that, in *Drosophila* Wind, five residues of the D-domain (Glu-212, Arg-215, Arg-218, Leu-219, and Leu-232) are essential for Pipe processing. Mutation of either Arg-215, Arg-218, or Leu-232 was sufficient to cause significant reduction in Pipe transport, whereas mutation of Glu-212 and Leu-219 had no significant effect unless combined (14). With the exception of Leu-232, these residues reside on α-helix 8 of the D-domain (Fig. 2). Together with Leu-232 on helix 9, the residues form a tight, surface-exposed cluster on the same face of the protein as the b-domain binding site (13). Surrounding residues do not seem to be involved (14).[4] Interestingly, work by Ma *et al.* (13) also shows that the D-domain of ERp29 could complement the corresponding domain in Wind. However, Mkrtchian and co-workers (19) have obtained a significantly different fold for the mammalian PDI-Dβ protein by NMR, leading us to ask whether the peptide binding site identified in the Wind protein is conserved in mammalian ERp29. We therefore studied the effects on Pipe protein translocation to the Golgi using 8 different mutants of the mouse ERp29 D-domain, based on the published Wind data (14).

In COS cells expressing both Pipe-GFP and Wind or one of its mutants, Golgi transport of Pipe signifies productive ER processing and functional integrity of the PDI-D protein. In cells expressing Pipe-GFP alone, the protein remains in the ER (Fig. 3, *panel a4*), as originally reported by Stein and co-workers (24), and relocates to the Golgi upon Wind coexpression (Fig. 3, *panels a1–a3*).

In the chimeric construct of the Wind b-domain and mouse ERp29 D-domain (Wind-b-p29D), mutation of any one of the corresponding residues (E222Q, R225A, K228E, L229S, and L242K) (Figs. 3 and 4) is sufficient to cause disruption of Pipe export to the Golgi. In Wind, no effect of the Wind E212Q mutation on Pipe transport was observed (14), requiring combination with the likewise tolerated L219S mutation for significant effect. In the chimeric construct, however, each mutation alone affects Pipe processing; the effect of the E222Q mutation is weak but visible, with ~15% of cells clearly showing ER-retained Pipe (Fig. 4, *panels c1–c3*), and the Wind-b-p9D-L229S mutant causes clear ER retention in at least 60% of the cells (Fig. 3, *panels h1–h3*). Similar levels (~60%) of ER-retained Pipe are observed with the mutants K228E and L242K (Fig. 3, *panels g1–g3* and *i1–i3*). The strongest effect is observed with the R225A mutant, which completely prevents ER export of Pipe (Fig. 3, *panels e1–e3*). The effects seen cannot be ascribed to

[4] M. Sevvana, G. M. Sheldrick, and D. M. Ferrari, manuscript in preparation.

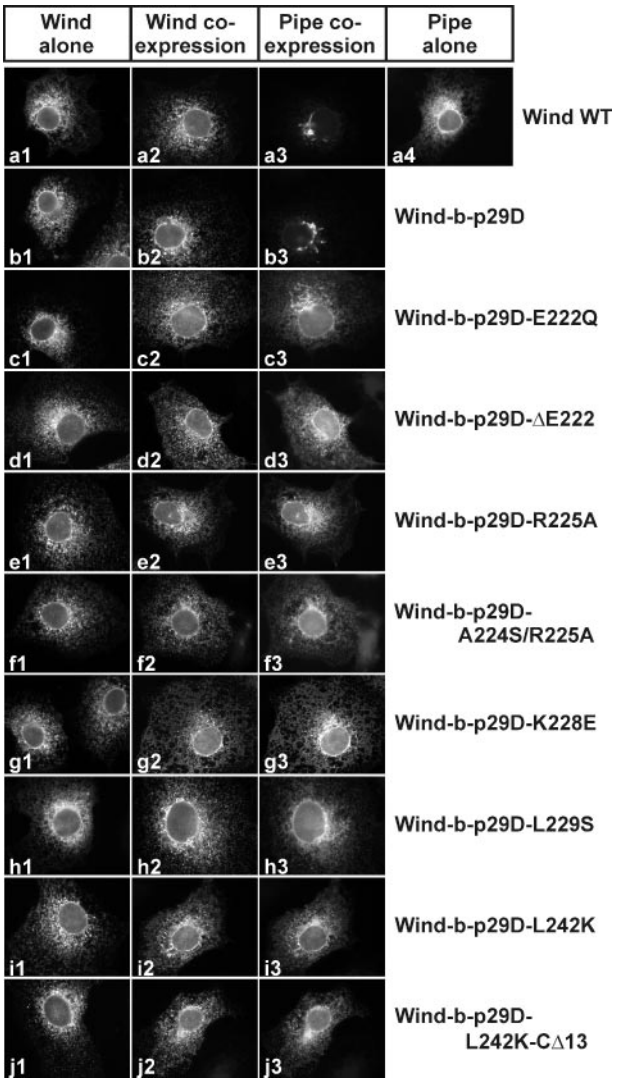

FIGURE 3. **Effect of D-domain mutants of Wind-b-p29D on Pipe export to the Golgi in COS cells.** The *first column* shows expression of WT Wind, Wind-b-p29D, or the indicated D-domain mutant alone, whereas the *second* and *third columns* show co-expressing cells stained for Wind and Pipe-GFP, respectively. Wind-b-p29D localizes to the ER when expressed alone (*b1*) or when co-expressed with Pipe-GFP (*b2*) and is capable of rerouting Pipe-GFP from the ER (*a4*) to the Golgi (*b3*) as expected, similar to WT Wind (*a1–a3*). In cells expressing mutants of the peptide-binding site of the D-domain, severe (ΔE222 (*d3*), R225A (*e3*), A224S/R225A (*f3*), and L242K-CΔ13 (*j3*)) or partial (E222Q (*c3*), K228E (*g3*), L229S (*h3*), and L242K (*i3*)) impairment of Pipe processing is observed. Partial impairment implies ER localization of Pipe in a significant number of (but not all) cells.

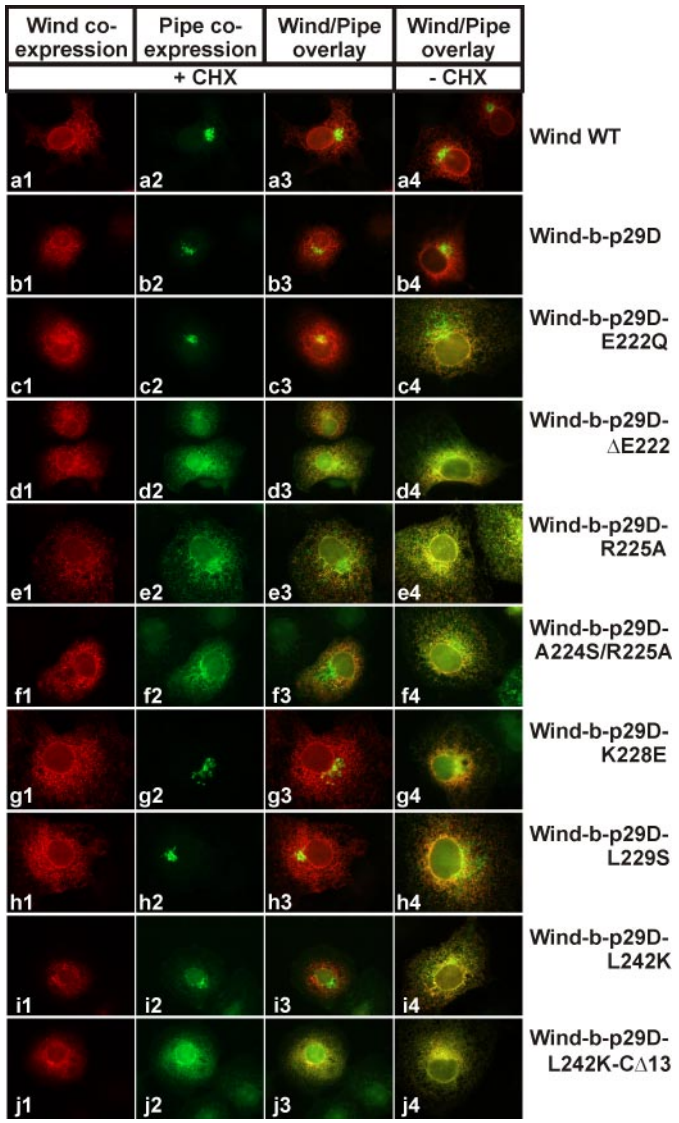

FIGURE 4. **Effect of D-domain mutants of Wind-b-p29D on Pipe export to the Golgi in co-expressing COS cells treated with cycloheximide.** Wind and Pipe-GFP staining are shown in the *first* and *second columns*, respectively, whereas the *third column* shows an overlay of the Wind and Pipe-GFP staining patterns within the same cell. Overlays of Wind and Pipe-GFP staining patterns in cells treated similarly but without cycloheximide (−*CHX*) are shown in the *fourth column*. Whereas the ER-retained staining pattern of Pipe-GFP in cells expressing mutants that severely impair transport (such as ΔE222 (*d3*), R225A (*e3*), A224S/R225A (*f3*), and L242K-CΔ13 (*j3*)) does not change when transfected cells are treated with cycloheximide, clear Golgi staining is visible in most cells expressing the weaker mutants (E222Q (*c3*), K228E (*g3*), L229S (*h3*) and L242K (*i3*)) after treatment with the drug. Golgi transport of Pipe in cells expressing WT Wind (*a3*) or Wind-b-p29D (*b3*) is not affected by cycloheximide treatment, as expected.

low protein expression or lack of ER retention, as each of the Wind-b-ERp29D mutants show high levels of expression when expressed alone and assume typical ER distribution patterns, even after 4 h of protein synthesis inhibition by cycloheximide (Fig. 4).

Interestingly, in co-expressing cells treated with cycloheximide for 4 h prior to fixation, Pipe transport to the Golgi is often seen to improve (Fig. 4), although Pipe localization, when expressed alone, is not affected by the drug (data not shown). In practically all cells expressing the mutants K228E and L229S (Fig. 4, *panels g1–g3* and *h1–h3*), Golgi localization is completely regained, and the same effect is seen with the weaker E222Q mutant (Fig. 4, *panels c1–c3*). For cells expressing Wind-b-p29-D-L242K, the proportion of cells with clearly ER-retained Pipe is halved, resulting in ~75% of co-expressing cells with Golgi-localized Pipe. In contrast, no effect of cycloheximide is observed in cells expressing the R225A mutant (Fig. 4, *panels e1–e3*).

To verify whether the integrity of the D-domain fold is essential for substrate processing, two mutants were constructed. The ΔE222 mutant removes a residue half-way into α-helix 8 and is expected to greatly destabilize this structure. Similarly, the L242K-NIL-CΔ13 mutant lacks the C-terminal 13 residues following α-helix 9, one of which (Phe-252) corresponds to

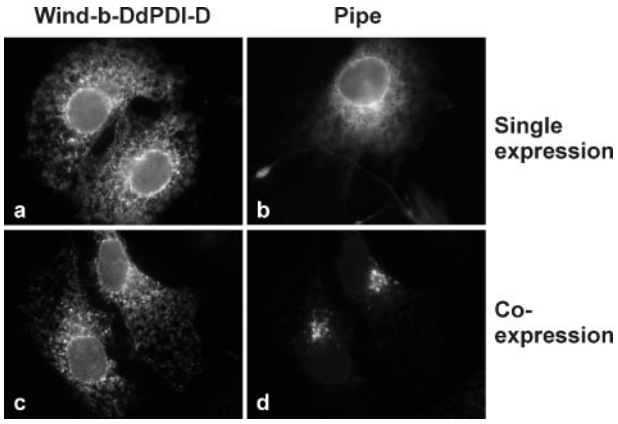

FIGURE 5. **The D-domain of a redox-active PDI can complement the Wind D-domain.** A chimera of the b-domain of Wind fused to the *D. discoideum* PDId D-domain is highly expressed in the ER of COS cells (*a* and *c*) and efficiently catalyzes Pipe relocation from the ER (*b*) to the Golgi (*d*).

Phe-242 of Wind, which is structurally important for the packing of helices 8 and 9 to the core of the D-domain. Both mutants completely prevent productive Pipe processing (Fig. 3, *panels d1–d3* and *i1–i3*), which are also in the presence of cycloheximide (Fig. 4, *panels d1–d3* and *i1–i3*), indicating that not only the conservation of binding site residues but also the integrity of the D-domain fold are important for substrate interaction.

The D-domain of a redox-active PDI protein can functionally replace the D-domain of Wind—The results above indicate that the D-domain of ERp29 contains a substrate binding site similar to that of Wind and suggests further similar functional properties. However, both proteins are members of the PDI-Dβ subclass of D-domain-containing proteins. Here, we chose to investigate whether the D-domain of the redox-active *D. discoideum* Dd-PDI protein (21, 22) might also functionally replace the D-domain of Wind.

As seen in Fig. 5, co-expression of Pipe with Wind-b-DdPDI-D fusion construct (Fig. 5, *c* and *d*) resulted in complete, efficient routing of Pipe to the Golgi. The Wind-b-DdPDI-D fusion construct, when expressed alone, asserted a typical ER distribution, as expected (Fig. 5*a*).

Biophysical Analysis of ERp29—To verify whether the effects of the ERp29 mutants on dimerization and function of the (chimeric) protein could be indirect with the main effect being protein malfolding and loss of secondary structure, several of the proteins were purified and analyzed by far UV circular dichroism.

For the dimerization mutants, mature WT ERp29, the single point mutants ERp29-D42N, ERp29-K52S, and the double mutant ERp29-D42N/K52S were analyzed. These proteins show highly similar far-UV circular dichroism spectra (Fig. 1*d*), indicating the presence of α-helices and β-sheets in all proteins. Loss of secondary structure is reflected in the spectrum for the partially heat-denatured (55 °C) WT protein, which served as a control. Importantly, these data prove that the proteins are well structured, that none of the proteins have altered amounts of random coil, and that loss of structure cannot be a significant factor in the effect of the mutations on protein dimerization.

For the functionally impaired D-domain mutants, mouse WT ERp29, the single point mutants ERp29-E222Q and

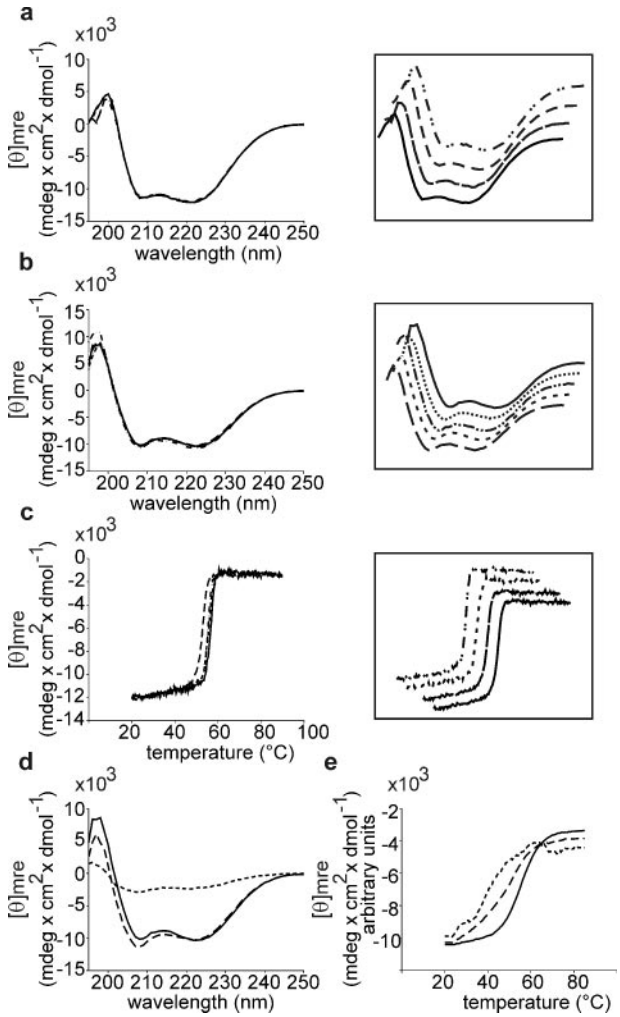

FIGURE 6. **Biophysical analysis of D-domain mutants of mammalian ERp29.** *a*, far-UV circular dichroism spectra of D-domain binding site mutants ERp29-E222Q (*long dashes*), ERp29-K228E (*short dashes*), and ERp29-R225A/G227S (*dash-dot*) compared with the WT full-length protein (*black*). Individual spectra are shown in the *boxed insets* and are staggered for ease of view. *b*, far-UV circular dichroism spectra of the single domain expression constructs D-E222Q (*dotted*), D-K228E (*short dashes*), D-L229S (*dash-dot*), and D-R225A (*long dashes*) compared with the WT D-domain construct (*black*). *c*, thermal denaturation curves of full-length D-domain mutants and the WT protein. ERp29-E222Q (*long dashes*), ERp29-K228E (*short dashes*), and ERp29-R225A/G227S (*dash-dot*) have denaturation curves very similar to that of the WT dimeric protein (*black*). *d*, two mutants designed to impact the overall structure and stability of the D-domain, D-ΔE222 (*long dashes*), and D-CΔ13 (*short dashes*) both show altered far-UV circular dichroism spectra compared with the WT D-domain construct (*black*). *e*, the single D-domain mutants D-ΔE222 (*long dashes*) and D-CΔ13 (*short dashes*) show thermal denaturation curves significantly dissimilar in slope, onset, and T_m from the WT D-domain construct (*black*), and their curves were normalized to the maximum negative mean residue ellipticity of the WT D-domain for comparison. Thermal denaturation was measured by plotting the mean residue ellipticities at 222 nm as a function of temperature using 0.5 °C increments.

ERp29-K228E, and the double mutant ERp29-R225A/G227S were analyzed. Furthermore, single domain D-domain constructs of WT mouse ERp29 (D-WT) and mutants D-ΔE222, D-E222Q, D-A224S/R225A, D-R225A, D-K228E, D-L229S, and D-CΔ13 were prepared and analyzed. Similar to the case for the dimerization mutants above, the full-length protein mutants ERp29-E222Q, ERp29-K228E, and ERp29-R225A/G227S (Fig. 6*a*) as well as the single domain expression constructs D-E222Q, D-K228E, D-L229S, and D-R225A (Fig. 6*b*)

all have far-UV circular dichroism spectra similar to the WT protein or D-domain alone, respectively. Thus, all of these mutants are likely well structured with no increase in the amounts of random coil, and above all, loss of structure is unlikely to be a significant factor in the effect of the mutations on protein function.

To verify the effects of each of the mutations on protein stability, far-UV circular dichroism measurements were made at 222 nm using a temperature gradient from 20–90 °C to cause progressive denaturation of the protein secondary structure elements. The mutants ERp29-D42N, ERp29-K52S, and ERp29-D42N/K52S show denaturation curves similar in shape and slope (except ERp29-D42N) to that of the WT protein (Fig. 1*e*), although with melting temperatures shifted from 55.6 °C by 6.6, 3.6, and 8.9 °C (data not shown). For ERp29-D42N, the slightly altered slope likely reflects the greater tendency of the protein to aggregate *in vitro* (data not shown), which is resolved in the ERp29-D42N/K52S double mutant. For all three mutant proteins, the unfolding process clearly occurs earlier than in the WT protein, consistent with the loss of a stabilizing dimerization interaction, without significant alteration to overall folding. Below 42 °C, all proteins are relatively stable.

The mouse D-domain mutants ERp29-E222Q, ERp29-K228E, and ERp29-R225A/G227S have denaturation curves very similar to that of the WT dimeric protein (Fig. 6*c*), with no significant changes to T_m except for the ERp29-E222Q mutant, which shows a T_m shift of 3.7 °C. This shift is not due to a loss of structure (see Fig. 6*b*) but could be explained by the loss of a putative salt bridge between Glu-222 and Arg-225. A possible salt bridge is visible in the Wind crystal structure (Protein Data Bank 1OVN; data not shown).

Finally, two mutants designed to impact the overall structure and stability of the D-domain, the single domain D-ΔE222 and D-CΔ13 proteins, both show far-UV circular dichroism spectra (Fig. 6*d*) and thermal denaturation curves at 222 nm (Fig. 6*e*), significantly dissimilar from the WT D-domain construct. This indicates an overall reduction in helical content as well as a significant decrease in protein stability for these proteins.

DISCUSSION

All species investigated apparently contain Wind orthologs (PDI-D proteins). However, although plants and yeast have *bona fide* disulfide redox activity because of the presence of thioredoxin a-type domains (PDI-Dα proteins), the orthologs in mammals and insects lack thioredoxin domain redox activity (PDI-Dβ proteins) (3), although as we have indicated (13, 25), they do contain surface-exposed cysteine residues.

Taken at face value, the similarities between the PDI-Dα and Dβ proteins are limited. Whereas PDI-Dα proteins generally have two a-type thioredoxin domains preceding the D-domain, PDI-Dβ proteins have a single b-type domain. PDI-Dα proteins generally lack classical ER retrieval signals (which PDI-Dβ proteins have) and use their D-domain for erd2-independent ER retention (21). PDI-Dα proteins have been shown, in contrast to PDI-Dβ proteins, to complement PDI-deficient yeast (13, 21). Finally, the overall similarity between the PDI-Dα and PDI-Dβ proteins is low (30% for human and slime mold PDI-D proteins), and varying three-dimensional structures have been proposed (a 1.9-Å crystal structure for Wind and an NMR structure of individual domains for rat ERp29 (19). Because of these differences, the general applicability of structural and functional findings from the Wind studies (13, 14) was unclear, and a characteristic role of PDI-D proteins based on their unique D-domains remained to be established. Here, we have provided data on the structure and function of PDI-D proteins, indicating conserved dimerization modes of PDI-Dβ proteins and structural and functional conservation of the D-domain with members of the PDI-Dα class.

Similar Dimerization Modes for the ERp29 and Wind b-Domains—Important residues at the dimerization interface of *Drosophila* Wind are conserved between human ERp29 and Wind proteins as well as in other PDI-Dβ proteins. Wind Gly-26, Val-28, Asp-31, and Arg-41, for instance, correspond to Gly-37, Leu-39, Asp-42, and Lys-52 in ERp29. Importantly, the critical dimer-stabilizing interactions mediated by Wind Val-28, Asp-31, and Arg-41 are mirrored in ERp29 by Leu-39, Asp-42, and Lys-52, mutants of which significantly reduce dimerization *in vitro*.

A different dimer model is suggested by Mkrtchian and colleagues (19), including residues that map to secondary structure elements on the opposite face of the protein. However, evidence in support of the predicted dimerization interface of rat ERp29 is not conclusive, as acknowledged by the authors (19). Using the mouse full-length protein mutants ERp29-R122S and D123A in our cross-linking assays, we found no evidence for such a dimerization site in mouse ERp29 (data not shown). However, both mutations led to severe aggregation of the protein, making any form of assessment impossible.

In contrast, our data is supported by far-UV circular dichroism analysis, which clearly shows that replacement of residues at the dimerization site leads to a shift in the thermal stability of the protein, consistent with the destabilization to be expected upon exposure of a mainly hydrophobic dimerization surface but with no loss of secondary structure content. We have thus shown that the dimerization interface of the b-domain of mammalian ERp29 probably resembles that of *Drosophila* Wind and encompasses residues within and around β1, α1, and α2. As dimerization has been reported for the fly (13), rat (26), and human (17) proteins, this mode of subunit association may well be a characteristic of PDI-Dβ proteins. Whether subunit association is required for the function of these proteins, as shown for Wind (14), remains to be demonstrated.

Mkrtchian and colleagues (19) suggest the presence of a multimerization site, defined by residues including Gly-67, Glu-68, Gly-97, and Asp-98. Extrapolation of these findings to the crystal structure of Wind places all four residues close to the peptide binding site of the b-domain (13), with Gly-87 and Glu-88 within the unique PDI-D loop. Although all of these residues can be replaced with no effect on substrate processing (13), at this time we can neither support nor disprove the suggestion that multimerization might utilize the identified residues. However, if this were the case, an interesting possibility of autoregulation of substrate access to the peptide binding site by steric occlusion upon multimerization arises and is certainly food for thought.

The D-domains of Both PDI-Dα and PDI-Dβ Proteins Are Likely Similar in Structure and Function to That of Drosophila Wind—We have defined a site within the D-domain of mouse ERp29 composed of non-contiguous residues from distinct structural elements, which is critical for substrate processing. Four of these residues, Glu-222, Arg-225, Lys-228, and Leu-229, reside in helix 8, whereas the fifth, Leu-242, is located within helix 9 of the D-domain. Replacement of any of these ERp29 residues reduces effective substrate processing, which is in excellent agreement with results from the corresponding experiments on Wind (14).

The severity of the disruptions caused by the D-domain mutations is apparent in our Pipe and Wind-b-p29D chimeric mutant co-expression system. In cells treated with cycloheximide, Golgi transport of Pipe is completely regained or improved for the mutants K228E and L229S, E222Q and L242K. This indicates that these mutants have a residual processing activity, the effect of which is only visible once continuous piling up of the large ER pool of Pipe is stopped with cycloheximide treatment. In contrast, the R225A mutation is more severe, leading to complete loss of processing activity.

Our results likely indicate a specific involvement of the residues in protein interaction, as neither of the mutants tested here (E222Q, R225A, K228E, nor L229S) cause any significant loss of secondary structure or stability *in vitro*. Furthermore, disruptive manipulation of the structure of the D-domain, either by removing a residue within helix 8 (ΔE222) or truncation of the protein at the end of helix 9 (CΔ13), causes complete loss of processing activity *in vivo* but, in contrast to the R225A mutant, clearly correlates with a loss of secondary structure and thermal stability *in vitro*. This indicates that the structural integrity of the 5-helix fold that comprises the D-domain is crucial for activity and, taken together with the conservation of and requirement for the five critical residues, suggests that the D-domains of the Wind and mouse orthologs have similar structures. Further support for this view is provided by the finding that the *Dictyostelium* Dd-PDI D-domain can efficiently replace the D-domain of Wind in our assays. Thus, these findings suggest a similar structure and function for the D-domain in both PDI-Dα and PDI-Dβ proteins, indicating that a likely characteristic feature of all D-domain proteins is the presence of a peptide binding site within the D-domain required for chaperone activity.

Finally, in our assays, we find no direct role for the linker Cys-159 in processing activity. Indeed, in the fusion construct of the Wind b-domain and the *Dictyostelium* Dd-PDI D-domain, the linker cysteine is eliminated with no adverse effect on protein stability or function. These data do not support an important structural role as suggested by others (20). However, Cys-157 in human ERp29, just as Cys-149 in Wind, is surface-exposed and readily oxidized (13, 25), and thus the presence of a conserved linker region Cys residue in PDI-Dβ proteins does indicate that it might be involved in interactions with other substrates.

Acknowledgments—We are grateful to the late H. D. Söling for assistance in constructing a Dictyostelium Dd-PDI D-domain fusion construct and R. Jakob for help in preparing the WT ERp29 D-domain construct. We also thank H. Reichardt and M. Möckel for excellent technical assistance. We are indebted to R. Jahn, G. Hasenfuss, and G. Fischer for their generous support.

REFERENCES

1. Anken, E., Braakman, I., and Craig, E. (2005) *Crit. Rev. Biochem. Mol. Biol.* **40,** 191–228
2. Trombetta, E. S., and Parodi, A. J. (2003) *Annu. Rev. Cell Dev. Biol.* **19,** 649–676
3. Ferrari, D. M., and Söling, H. D. (1999) *Biochem. J.* **339,** 1–10
4. Freedman, R. B., Klappa, P., and Ruddock, L. W. (2002) *EMBO Rep.* **3,** 136–140
5. Ellgaard, L., and Ruddock, L. W. (2005) *EMBO Rep.* **6,** 28–32
6. Kleizen, B., and Braakman, I. (2004) *Curr. Opin. Cell Biol.* **16,** 343–349
7. Molinari, M., Eriksson, K. K., Calanca, V., Galli, C., Cresswell, P., Michalak, M., and Helenius, A. (2004) *Mol. Cell* **13,** 125–135
8. Mayer, M., Reinstein, J., and Buchner, J. (2003) *J. Mol. Biol.* **330,** 137–144
9. Gething, M. J. (1999) *Semin. Cell Dev. Biol.* **10,** 465–472
10. Darby, N. J., and Creighton, T. E. (1995) *Biochemistry* **34,** 11725–11735
11. Darby, N. J., Penka, E., and Vincentelli, R. (1998) *J. Mol. Biol.* **276,** 239–247
12. Klappa, P., Ruddock, L. W., Darby, N. J., and Freedman, R. B. (1998) *EMBO J.* **17,** 927–935
13. Ma, Q., Guo, C., Barnewitz, K., Sheldrick, G. M., Söling, H.-D., Usón, I., and Ferrari, D. M. (2003) *J. Biol. Chem.* **278,** 44600–44607
14. Barnewitz, K., Guo, C., Sevvana, M., Ma, Q., Sheldrick, G. M., Söling, H.-D., and Ferrari, D. M. (2004) *J. Biol. Chem.* **279,** 39829–39837
15. Pirneskoski, A., Klappa, P., Lobell, M., Williamson, R. A., Byrne, L., Alanen, H. I., Salo, K. E. H., Kivirikko, K. I., Freedman, R. B., and Ruddock, L. W. (2004) *J. Biol. Chem.* **279,** 10374–10381
16. Russell, S. J., Ruddock, L. W., Salo, K. E. H., Oliver, J. D., Roebuck, Q. P., Llewellyn, D. H., Roderick, H. L., Koivunen, P., Myllyharju, J., and High, S. (2004) *J. Biol. Chem.* **279,** 18861–18869
17. Ferrari, D. M., Nguyen Van, P., Kratzin, H. D., and Söling, H. D. (1998) *Eur. J. Biochem.* **255,** 570–579
18. Sargsyan, E., Baryshev, M., Szekely, L., Sharipo, A., and Mkrtchian, S. (2002) *J. Biol. Chem.* **277,** 17009–17015
19. Liepinsh, E., Baryshev, M., Sharipo, A., Ingelman-Sundberg, M., Otting, G., and Mkrtchian, S. (2001) *Structure* (*Lond.*) **9,** 457–471
20. Hermann, V. M., Cutfield, J. F., and Hubbard, M. J. (2005) *J. Biol. Chem.* **280,** 13529–13537
21. Monnat, J., Neuhaus, E. M., Pop, M. S., Ferrari, D. M., Kramer, B., and Soldati, T. (2000) *Mol. Biol. Cell* **11,** 3469–3484
22. Monnat, J., Hacker, U., Geissler, H., Rauchenberger, R., Neuhaus, E. M., Maniak, M., and Soldati, T. (1997) *FEBS Lett.* **418,** 357–362
23. Gasteiger, E., Hoogland, C., Gattiker, A., Duvaud, S., Wilkins, M. R., Appel, R. D., and Bairoch, A. (2005) in *The Proteomics Protocols Handbook* (Walker, J. M., ed) pp. 571–607, Humana Press, Hatfield, UK
24. Sen, J., Goltz, J. S., Konsolaki, M., Schupbach, T., and Stein, D. (2000) *Development* (*Camb.*) **127,** 5541–5550
25. Ferrari, D. M. (1999) *Isolation and Characterisation of a Novel Protein Disulphide Isomerase (PDI)-related Protein, ERp28: Implications for the PDI family*, Cuvillier Verlag, Goettingen, Germany
26. Mkrtchian, S., Baryshev, M., Matvijenko, O., Sharipo, A., Sandalova, T., Schneider, G., Ingelman-Sundberg, M., and Mkrtchiana, S. (1998) *FEBS Lett.* **431,** 322–326